Do Upslope Impervious Surfaces Impact the Run-on/Runoff Relationship?

Elizabeth A. Pappas[1]; Chi-hua Huang[2]; and James V. Bonta, M.ASCE[3]

Abstract: As a watershed is urbanized, characteristics of runoff from new upslope impervious surfaces may differ from runoff generated on the predevelopment soil surface in quantity, time of concentration, and sediment load. This may cause changes to the erosion regime on downslope soil surfaces. We simulated rainfall at three rates (20, 30, 40 mm/h) to generate runoff from 0.6 m^2 boxes. Boxes were either treated with an impervious surface or filled with soil 0.2 m deep and were connected together in series of four boxes along the 4-m slope to produce different arrangements of impervious and pervious soil surfaces (0, 25, 50% impervious) and under different antecedent soil moisture conditions. Results indicate that previously established numerical models predicting runoff characteristics as a function of run-on characteristics generate good correlations at 0% imperviousness, but these correlations become insignificant as imperviousness increases. Imperviousness significantly influenced sediment regime, suggesting that some previously established equations relating soil erosion to run-on characteristics cannot be simply applied to areas where runoff production occurs on surfaces having an impervious component.
DOI: 10.1061/(ASCE)HE.1943-5584.0000325.

CE Database subject headings: Urban development; Stormwater management; Soil erosion; Runoff.

Author keywords: Urbanization; Impervious surface; Stormwater management; Soil erosion.

Introduction

As previously natural or agricultural landscapes are developed for urban and suburban uses, much of the pervious soil surface is replaced with impervious surfaces such as rooftops, parking lots, and transportation surfaces. The increased extent of impervious surface typically shifts the landscape from an infiltrative sink for rainfall to a source of runoff (Booth and Jackson 1997). Runoff and sediment leaving new upslope impervious surfaces may differ from the predevelopment condition, with possible impact to the erosion regime on downslope soil surfaces. By this mechanism, the characteristics of run-on to existing downslope erodible surfaces are altered. The importance of run-on in downslope hydrology has been previously considered (Smith and Hebbert 1979; Woolhiser et al. 1996; Corradini et al. 1998; Nahar et al. 2004), but rainfall-runoff studies largely ignore this parameter. Moreover, erosion monitoring data collected over the course of increasing urban and suburban development are scarce, attributable in part to the logistical difficulties associated with watershed monitoring over the longer term required to characterize hydrologic and erosional impacts at several stages throughout the development process. Additionally, there are few experimental data to show how changes in run-on water and sediment concentration affect erosion processes downslope (Zheng et al. 2000), since most data are collected at the outlet, representing integration in space and time over flow pathways and sampling intervals (Huang et al. 1999). For these reasons and because the direct effects of imperviousness seem intuitive (Terstriep et al. 1976), models have generally been used to better understand or determine the subsequent impacts of impervious surface on hydrology (O'Loughlin et al. 1996), with debated accuracy. The primary objective of this study was to experimentally determine whether the replacement of upslope soil with impervious surfaces impacts the relationship of downslope runoff and erosion as a function of run-on characteristics.

[1]Research Hydraulic Engineer, U.S. Dept. of Agriculture, Agricultural Research Service, National Soil Erosion Research Laboratory, 275 S. Russell St., West Lafayette, IN 47907.

[2]Research Leader, U.S. Dept. of Agriculture, Agricultural Research Service, National Soil Erosion Research Laboratory, 275 S. Russell St., West Lafayette, IN 47907.

[3]Supervisory Research Hydraulic Engineer, U.S. Dept. of Agriculture, Agricultural Research Service, North Appalachian Experimental Watershed, PO Box 488, Coshocton, OH 43812.

Note. This manuscript was submitted on October 1, 2009; approved on August 21, 2010; published online on September 15, 2010. Discussion period open until September 1, 2011; separate discussions must be submitted for individual papers. This paper is part of the ***Journal of Hydrologic Engineering***, Vol. 16, No. 4, April 1, 2011. ©ASCE, ISSN 1084-0699/2011/4-345–350/$25.00.

Materials and Methods

Treatments

Runoff and sediment losses from sloped plots having various upslope impervious cover were measured. Each plot consisted of four segments of 1-m length, having either a soil surface (S) or impervious cover (I). Treatments are denoted in upslope to downslope sequence as SSSS (0% upslope imperviousness), ISSS (50% upslope imperviousness) and IISS (100% upslope imperviousness). Three replications of each treatment were performed under two different initial soil moisture content levels (θ_{vi}): dry ($15\% < \theta_{vi} < 17\%$), and wet ($20\% < \theta_{vi} < 24\%$).

Experimental Apparatus

A cascade of four sloped soil boxes described by Pappas et al. (2008) and Shuster et al. (2008) was used for rainfall simulations (Fig. 1). The two upslope boxes were always connected to each other and are considered run-on contributors to the two downslope soil boxes, which were always connected to each other, such that two sampling points were used. Each S box was filled with a moderately well drained Oxyaquic Dystrudept silt loam (34.0% sand, 51.5% silt, 14.5% clay). Each I box was made with a sheet metal

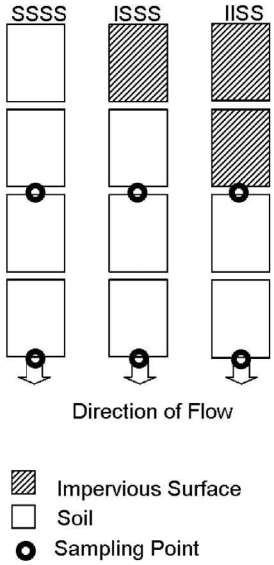

Fig. 1. Soil box rainfall simulation layout representing three treatments: SSSS (no impervious cover), ISSS (upslope area is 50% impervious), and IISS (upslope area is 100% impervious)

cover coated with spray-on truck bed liner in order to shed water similarly to smooth asphalt. Each soil box was 1 m long, 60 cm wide, and 20 cm deep (soil depth). Boxes were arranged on a 5% slope so that surface runoff and sediment flowed from upslope soil boxes into downslope soil boxes through short baffled flumes in the connected position, while hinged interbox sampling devices allowed intermittent sampling of runoff and sediment between the upslope contributor boxes and the downslope erosion study boxes. Soil was allowed to freely drain through holes in the bottom of the soil boxes.

Before each rainfall event, soil boxes were prepared by drying soil to an average volumetric moisture content of 16%, sieving to ≤ 2 cm, and packing each box to a bulk density of $1.25\ \mathrm{g/cm^3}$. The soil cover was then graded with a hand trowel. To minimize effects from variability in surface packing, a prewetting rain of 10 mm/h for a duration of 45 min was applied and the soil boxes were then left to equilibrate for 24 h. Average prepared initial volumetric soil moisture (θ_{vi}) was 16% for dry treatments. Without further surface manipulation or preparation, rainfall simulations were repeated for wet treatments 72 h after dry treatment rainfall simulations were completed. Average θ_{vi} was 22% for wet treatments. Soil moisture was measured by specific capacitance probes installed horizontally in each box at the 7- and 13-cm depths. Measurements were recorded hourly before and after rainfall simulations and every 2 min during rainfall simulation. Maximum observed volumetric soil moisture contents occurred at 96 min at the 7-cm depth (the end of the rainfall simulation), and at 70 h at the 13-cm depth. Soil moisture was not found to exceed 33% for any depth or treatment. Therefore, it is unlikely that depth boundary effects were significant.

Rainfall Simulation

A programmable oscillating nozzle rainfall simulator was used to generate desired rainfall patterns for all trials. Vertical distance between the nozzles and the soil cover was approximately 2.5 m, and nozzle pressure was 41.4 kPa. The water source was deionized. Rainfall was applied at 20 mm/h for 48 min, then 30 mm/h for 24 min, and 40 mm/h for 24 min. Rain gauges were deployed to correspond with each soil box. The average absolute value of deviation from designed rainfall was 9%. No pattern was detected with regard to distribution of positive and negative deviations. Rainfall sequence was based on preliminary trials and designed to generate runoff at several rates and reach steady-state at multiple rainfall intensities.

Sampling

Two sampling regimes were used. In the first, every four minutes, timed 1 min runoff samples were collected in 1-L Nalgene bottles from the entire slope length with all four boxes in the connected position. The second sampling regime was staggered from the first by 2 min. The upslope section was disconnected from the downslope section every four minutes to obtain timed, 1 min runoff samples from between the upslope and downslope sections and from the end of the downslope section, simultaneously. The purpose of the second midslope sampling was to collect the data necessary to determine run-on characteristics to the downslope area and prevailing sediment regimes. Previous research has shown that 30 s equilibration periods after interbox samplers were opened and before intermediate and remainder sampling, and after interbox samplers were closed and before sampling from the entire plot connected is sufficient to remove measurement impacts attributable to the connection and disconnection of boxes. With this procedure, differences in sediment loss rate measurements caused by the mechanics of the interbox samplers were found to be negligible (Pappas et al. 2008).

Sample Processing

Samples and container tare weights were recorded to the nearest 0.01 g. Then 3–5 mL of saturated alum solution [$AlK(SO_4)_2$] was added to each sample to flocculate suspended sediment. After a 12 to 18 h settling period at room temperature, samples were decanted and dried at 105°C to a constant weight.

Calculations

Runoff volumes were determined for each sample by gravimetric methods using the difference between the weight of the total sample and the weight of the dried bottle and sediment. Runoff and sedimentation rates were determined for each sample interval by dividing respective weights by the sampling duration. Average upslope steady-state runoff and sediment losses (S_U) were determined using samples collected between the two upslope and the two downslope boxes and averaging their sediment loss rates after steady-state erosion had been reached at the present rainfall intensity. Average downslope steady-state runoff and sediment losses (S_D) were determined using samples collected at the end of the four-box slope length but while the two upslope soil boxes were disconnected from the two downslope soil boxes. For the entire plot (S_{UD}), samples collected at the end of the four-box slope length, while all soil boxes were connected, were used. All statistical analyses were performed using JMP 7.0 (manufactured by SAS Institute Inc., Cary, NC).

Results and Discussion

Sediment Regimes

Table 1 gives S_U, S_D, and S_{UD} values for SSSS, ISSS, and IISS configurations at each rainfall intensity. Corresponding values are considered to be equal if they are not significantly different ($\alpha = 0.1$). Highest sediment run-on rates were observed in the ISSS plots, while S_U on IISS plots, which was generated on entirely

Table 1. Average Steady-State Sediment Loss Rates from Upslope and Downslope (S_U and S_D) Components and Both Together (S_{UD}) from Plots under Low and High Initial Soil Moisture Content (θ_{vi})

Rainfall rate (mm/h)	Sediment loss rate (g/min)							
	$(15\% < \theta_{vi} < 17\%)$				$(20\% < \theta_{vi} < 24\%)$			
	S_U	S_D	$S_U + S_D$	S_{UD}	S_U	S_D	$S_U + S_D$	S_{UD}
				SSSS				
20	1.2	1.2	2.4	1.6	2.0	1.4	3.4	2.4
30	3.0	2.8	5.8	5.7	4.7	3.5	8.2	7.8
40	6.3	5.2	11.5	12.4	8.2	6.5	14.6	14.1
				ISSS				
20	1.5	0.8	2.3	2.0	2.0	0.9	2.9	1.8
30	4.6	2.2	6.8	3.6	5.1	2.6	7.8	5.2
40	8.2	3.7	12.0	8.8	9.8	5.3	15.1	11.0
				IISS				
20	0.0	0.3	0.3	0.7	0.0	1.5	1.5	3.0
30	0.0	1.1	1.1	2.8	0.0	3.7	3.7	8.5
40	0.0	2.5	2.5	5.8	0.0	5.8	5.8	14.0

impervious surfaces, was without sediment. Highest overall sediment loss rates were observed from the SSSS plots (maximum 14.1 g/min) although if only erodible surface area is considered, then the SSSS plots produced the lowest sediment loss flux. According to concepts presented by Ellison and Ellison (1947a, b) and Meyer and Wischmeier (1969), sediment transport is limited either by detachment processes or by transport capacity. In this case, erosion is limited by transport where $S_{UD} \leq S_U$ (Aksoy and Kavvas 2005), as is the case in the low θ_{vi} ISSS plots under 30 and 40 mm/h rainfall and in the high θ_{vi} ISSS plots at 20 and 30 mm/h. We surmise that under 40 mm/h rainfall, significantly higher water runoff rates on the high θ_{vi} ISSS plots led to an increase in transport capacity.

Simple rules for determining sediment regime were proposed by Huang et al. (1999). Adapted for this study, the relationships between sediment losses from the upslope area alone, from the downslope area alone, and from the downslope area while receiving run-on from the upslope area are used to determine which of five possible sediment regimes dominate (Table 2). By applying Huang's test (Huang et al. 1999), we determine that Rule 3 applies to SSSS surfaces at the lowest rainfall intensity (20 mm/h), but Rule 4 applies at the subsequent 30 and 40 mm/h rainfall intensities. This indicates a shift in sediment regime from erosion in excess of deposition to equilibrium over the course of the rainfall simulation.

Slopes having an upslope area that was partially impervious (ISSS) received the highest sediment run-on rates (Table 1) and exhibited the most complex and dynamic sediment regime. When initial soil moisture was low, sediment regime was described by Rule 3 at 20 mm/h rainfall intensity, and shifted to Rule 1, and then to Rule 2 with increases in rainfall intensity. This indicates a shift from erosion in excess of deposition, to deposition in excess of erosion, and then finally to erosion equal to deposition. Under the higher initial soil moisture regime, the ISSS sediment regime shifted from deposition in excess of erosion, to deposition equal to erosion, and finally to erosion in excess of deposition with increasing rainfall intensity.

Table 2. Rules for Determining Dominant Sediment Regime as Proposed by Huang et al. (1999)

	Rule	Dominant sediment regime
1	$S_{UD} < S_U$	Deposition in excess of erosion
2	$S_{UD} = S_U$	Deposition equal to erosion
3	$S_U < S_{UD} < (S_{U+}S_D)$	Erosion in excess of deposition
4	$S_{UD} = (S_{U+}S_D)$	Equilibrium; no run-on effects
5	$S_{UD} > (S_{U+}S_D)$	Run-on water causes increased downslope erosion

Slopes having entirely impervious upslope surfaces (IISS) yielded higher sediment losses with the upslope impervious surface connected to the downslope soil surface than with the components disconnected (Table 1). This was expected since sediment-free runoff generated on the upslope impervious surface contributed to a higher runoff rate on the downslope soil surface and would naturally increase sediment detachment and transport. In fact, since S_U was always a zero value for IISS, Rule 5 always applied, indicating that this run-on water caused increased downslope erosion.

Significant Correlations

Previous researchers have developed simple numeric models relating sediment runoff rate to water runoff rate by a power equation (Band 1985; Mathier et al. 1989; Huang and Bradford 1993; Mathier and Roy 1996). Huang and Bradford (1993) also found water runoff rate to be related to sediment runoff rate using a second-order polynomial model in some cases. Others have found runoff sediment rate to be related to run-on water rate and, to a lesser extent, run-on sediment rate (Zheng et al. 2000). Using these equations, we found no significant correlations between run-on water, runoff water, or run-on sediment rates and runoff sediment or net runoff sediment rates when examining the data from SSSS, ISSS, and IISS together (Table 3). However, our finding that sediment regime is influenced by impervious treatment was confirmed by statistical analysis, which indicates distinctly different correlations between run-on characteristics and runoff sediment rates depending on upslope impervious treatment for SSSS and ISSS (Table 4). This finding and our related equation parameters are unique to our experimental conditions. Because erosion processes are soil and scale-dependent, these cannot simply be extrapolated to larger scale urban areas. However, our findings suggest that imperviousness may be a confounding factor in the simple sediment loading predictive models under some conditions. No significant

Table 3. Statistical Parameters for Regression Equation as a Power Function Where the Dependent Variable Is Runoff Sediment Rate: Equation of the Form $Y = Ax^B$

Independent Variable	Grouping	R^2	P	A	B
Run-on water rate	IISS	0.53	< 0.0006	0.0000075	1.9601
Run-on water rate[a]	ISSS	0.88	< 0.0001	0.000041	1.8377
Run-on water rate[a]	SSSS	0.86	< 0.0001	0.00012	1.7445
Run-on water rate	None	0.51	< 0.0001	0.062	1.5685
Runoff water rate	IISS	0.56	0.0003	0.00081	1.2138
Runoff water rate[a]	ISSS	0.85	< 0.0001	0.00010	1.5606
Runoff water rate[a]	SSSS	0.97	< 0.0001	0.000018	1.8518
Runoff water rate	None	0.78	< 0.0001	0.000061	1.6486

[a]The x, y fit is considered significant, and equation parameters are listed where $R^2 > 0.8$ and $P < 0.05$.

Table 4. Statistical Parameters for Regression Equation as a Second-Order Polynomial Function Where the Dependent Variable Is Runoff Sediment Rate

Independent variable	Grouping	R^2	P	A	B	C
Run-on sediment rate	IISS	N/A[b]	N/A[b]	N/A	N/A	—
Run-on sediment rate[a]	ISSS	0.81	< 0.0001	0.13	−0.0539	1.5697
Run-on sediment rate[a]	SSSS	0.96	< 0.0001	0.16	3.6279	−2.5353
Run-on sediment rate	None	0.75	< 0.0001	1.5	1.0460	—

[a]The x, y fit is considered significant, and equation parameters are listed where $R^2 > 0.8$ and $P < 0.05$.
[b]Run-on sediment rate is always zero.

correlations were observed between run-on characteristics and runoff sediment rate for IISS, which received no run-on sediment load.

It can be seen in Fig. 2 that the correlation equations relating run-on water rate to sediment runoff rate for SSSS and ISSS are unique where the shaded confidence intervals do not overlap. This represents the interval between water run-on rate = 320 and 800 mL/min. There was no significant correlation for IISS. Likewise, Fig. 3 illustrates unique correlation equations for sediment runoff rates as a function of water runoff rates from SSSS and ISSS for water runoff rate values > 650 mL/min. Again, no significant correlation was observed for IISS.

Where sediment run-on is the independent variable, we chose a second-order polynomial model. This is supported by the theory that maximum erosion occurs when the flow contains an optimum amount of sediment to initiate detachment to the extent of transport capacity, whereas erosion will decrease if the run-on has insufficient sediment to initiate detachment or has sediment close to or in excess of transport capacity (Ellison and Ellison 1947a, b). According to Fig. 4, the SSSS and the ISSS treatment exhibit distinctly unique correlations between sediment run-on rate and sediment runoff rate for sediment run-on rates > 2.0 and < 7.8 g/min, whereas IISS had no upslope sediment and therefore no sediment run-on.

Because we expect soil deposition to occur over some ranges of water run-on and runoff, resulting in negative net sediment runoff values, we also chose a second-order polynomial model in which

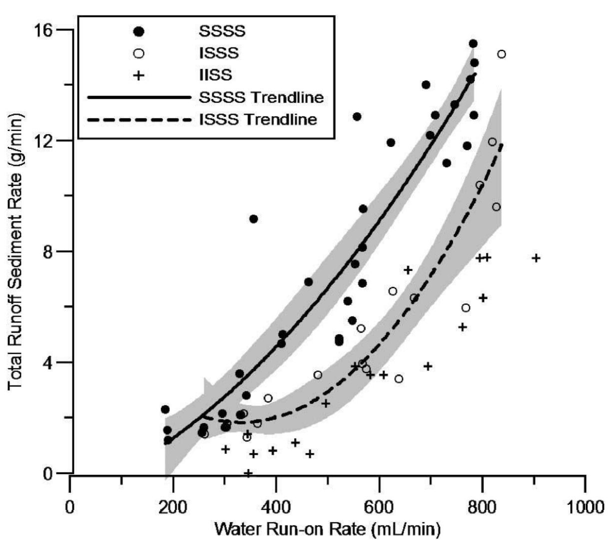

Fig. 2. Steady-state sediment runoff rates as a function of water run-on rate. Shaded areas indicate predicted confidence intervals ($\alpha = 0.05$). Trend lines and confidence intervals are displayed only where $R^2 > 0.8$ and $P < 0.05$ (SSSS and ISSS)

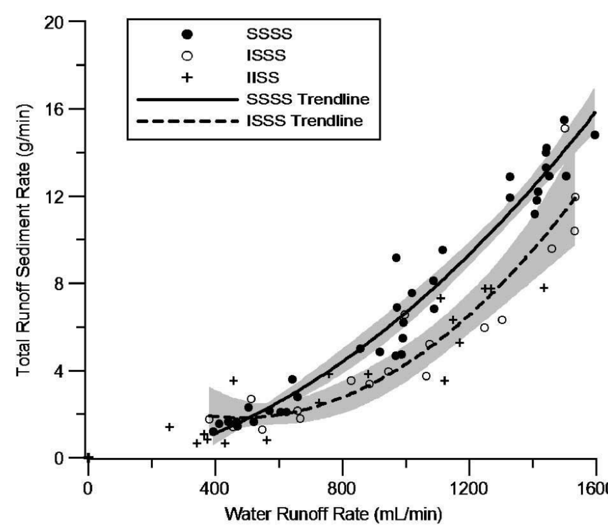

Fig. 3. Steady-state sediment runoff rates as a function of water runoff rate. Shaded areas indicate predicted confidence intervals ($\alpha = 0.05$). Trend lines and confidence intervals are displayed only where $R^2 > 0.8$ and $P < 0.05$ (SSSS and ISSS)

our dependent variable was net sediment runoff. Run-on characteristics were significantly correlated with net sediment runoff rates only for the SSSS treatment (Table 5), and all lines of fit are illustrated in Figs. 5–7. As we saw in our sediment regime analysis, negative net sediment runoff rates (deposition) were observed only from the ISSS treatment, which had the highest sediment run-on rates. While the variability in the ISSS data set was high and no significant correlation was observed relating water run-on to net sediment runoff, an unusual trend was observed. At low levels of water run-on, no net erosion or deposition was observed, but as water run-on rate increased, sediment run-on also increased, and deposition occurred in the downslope boxes. Increasing the water run-on rate further seemed to result in the detachment and transport of these sediments.

Conclusions

Many modern-day urban fringe landscapes are in a state of increasing imperviousness. Sediment regimes and erosion responses to hydrology and run-on characteristics in landscapes having significant areas of impervious surfaces are not well understood. A novel, serial soil box system was used under rainfall simulation to characterize the response of sediment losses to characteristics of run-on generated on upslope surfaces having different levels of imperviousness. Results indicate that under our experimental conditions, impervious treatment influenced the prevailing sediment regimes and the observed correlations between run-on characteristics and runoff sediment losses, as well as the observed correlations between water runoff rate and sediment runoff rate. We found that applying increasing levels of imperviousness to previously

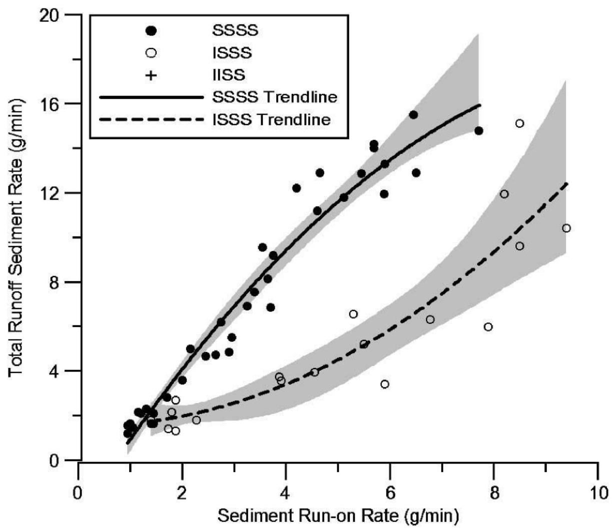

Fig. 4. Steady-state sediment runoff rates as a function of sediment run-on rate. Shaded areas indicate predicted confidence intervals ($\alpha = 0.05$)

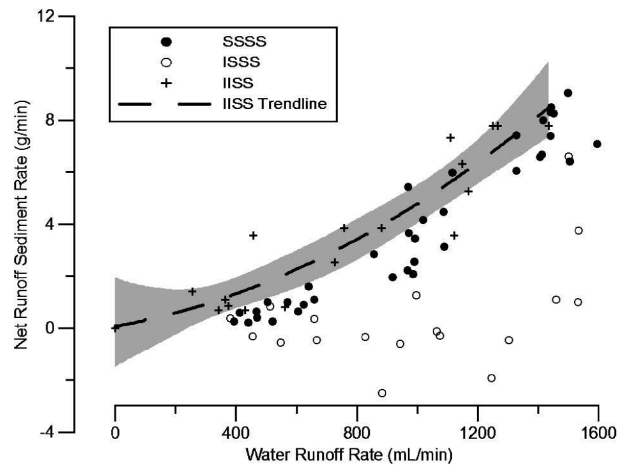

Fig. 6. Steady-state net sediment runoff rates as a function of water runoff rate. Shaded areas indicate predicted confidence intervals ($\alpha = 0.05$). Trend lines and confidence intervals are displayed only where $R^2 > 0.8$ and $P < 0.05$ (SSSS)

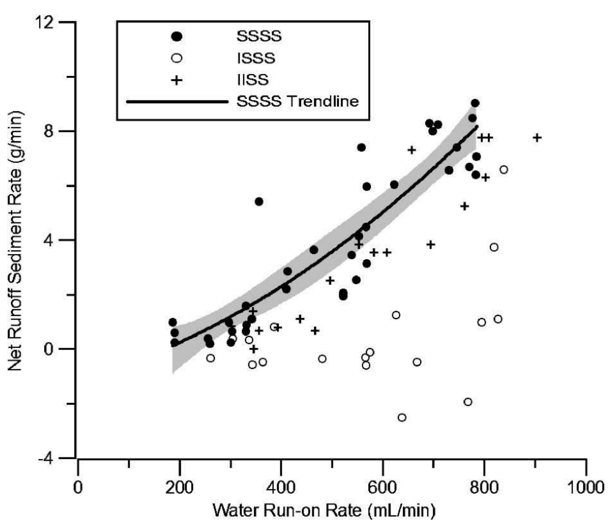

Fig. 5. Steady-state net sediment runoff rates as a function of water run-on rate. Shaded areas indicate predicted confidence intervals ($\alpha = 0.05$). Trend lines and confidence are displayed only where $R^2 > 0.8$ and $P < 0.05$ (SSSS)

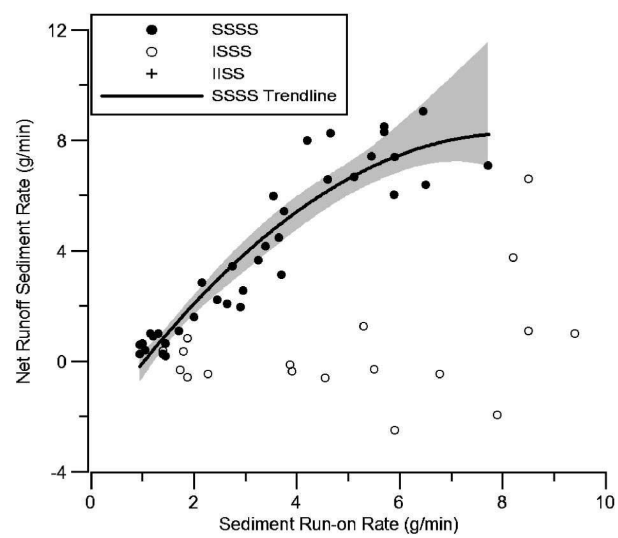

Fig. 7. Steady-state net sediment runoff rates as a function of sediment run-on rate. Shaded areas indicate predicted confidence intervals ($\alpha = 0.05$). Trend lines and confidence intervals are displayed only where $R^2 > 0.8$ and $P < 0.05$ (SSSS)

Table 5. Statistical Parameters for Regression Equation as a Second-Order Polynomial Function Where the Dependent Variable Is Net Runoff Sediment Rate: Equation of the Form $Y = Ax^2 + Bx + C$

Independent variable	Grouping	R^2	P	A	B	C
Run-on water rate	IISS	0.52	0.0038			
Run-on water rate	ISSS	0.39	0.0241			
Run-on water rate[a]	SSSS	0.82	< 0.0001	0.0000090	0.0051	−1.1157
Run-on water rate	None	0.35	< 0.0001			
Runoff water rate	IISS	0.64	0.0005			
Runoff water rate	ISSS	0.46	0.01			
Runoff water rate[a]	SSSS	0.91	< 0.0001	0.0000030	0.0021	−1.1686
Runoff water rate	None	0.49	< 0.0001			
Run-on sediment rate	IISS	N/A[b]	N/A[b]			
Run-on sediment rate	ISSS	0.25	0.1052			
Run-on sediment rate[a]	SSSS	0.88	< 0.0001	0.16	2.6280	−2.5357
Run-on sediment rate	None	0.29	0.0001			

[a]The x, y fit is considered significant, and equation parameters are listed where $R^2 > 0.8$ and $P < 0.05$.
[b]Run-on sediment rate is always zero.

established simple numerical models (either power or second-order polynomial equations) resulted in decreasing goodness of fit. For this reason, these previously established equations used in predicting erosion as a function of run-on characteristics or runoff rates may not be directly applicable to urbanizing areas of heterogeneous imperviousness. We anticipate that specific local soil conditions and scale will influence the applicability of this finding.

Acknowledgments

The writers gratefully recognize the contributions and technical support of Janae Bos in the implementation of this research.

References

Aksoy, H., and Kavvas, M. L. (2005). "A review of hillslope and watershed scale erosion and sediment transport models." *Catena*, 64, 247–271.

Band, L. (1985). "Field parameterization of an empirical sheetwash transport equation." *Catena*, 12(4), 281–290.

Booth, D. B., and Jackson, C. R. (1997). "Urbanization of aquatic systems: Degradation thresholds, stormwater detention, and limits of mitigation." *J. Am. Water Resour. Assoc.*, 33, 1077–1090.

Corradini, C., Morbidelli, R., and Melone, F. (1998). "On the interaction between infiltration and Hortonian runoff." *J. Hydrol. (Amsterdam)*, 204, 52–67.

Ellison, W. D., and Ellison, O. T. (1947a). "Soil erosion studies: Part VI: Soil detachment by surface flow." *Agric. Eng.*, 28, 402–408.

Ellison, W. D., and Ellison, O. T. (1947b). "Soil erosion studies: Part VII: Soil transportation by surface flow." *Agric. Eng.*, 28, 442–450.

Huang, C., and Bradford, J. M. (1993). "Analyses of slope and runoff factors based on the WEPP erosion model." *Soil Sci. Soc. Am. J.*, 57, 1176–1183.

Huang, C., Wells, L. K., and Norton, L. D. (1999). "Sediment transport capacity and erosion processes: Model concepts and reality." *Earth Surf. Processes Landforms*, 24, 503–516.

Mathier, L., and Roy, A. G. (1996). "A study on the effect of spatial scale on the parameters of a sediment transport equation for sheetwash." *Catena*, 26(3/4), 161–169.

Mathier, L., Roy, A. G., and Pare, J. P. (1989). "The effect of slope gradient and length on the parameters of a sediment transport equation for sheetwash." *Catena*, 16(6), 545–558.

Meyer, L. D., and Wischmeier, W. H. (1969). "Mathematical simulation of the process of soil by water." *Trans. ASAE*, 12, 754–758.

Nahar, N., Govindaraju, R. S., Corradini, C., and Morbidelli, R. (2004). "Role of run-on for describing field-scale infiltration and overland flow over spatially variable soils." *J. Hydrol. (Amsterdam)* 286, 36–51.

O'Laughlin, G., Huber, W., and Chocat, H. (1996). "Rainfall-runoff processes and modeling." *J. Hydraul. Res.*, 34(6), 733–751.

Pappas, E. A., Smith, D. R., Huang, C., Shuster, W. D., and Bonta, J. V. (2008). "Impervious surface impacts to runoff and sediment discharge under laboratory rainfall simulation." *Catena*, 72, 146–152.

Shuster, W. D., Pappas, E. A., and Zhang, Y. (2008). "A laboratory-scale simulation of runoff response from pervious-impervious systems." *J. Hydrol. Eng.*, 13(9), 886–893.

Smith, R. E., and Hebbert, R. H. B. (1979). "A Monte Carlo analysis of the hydrologic effects of spatial variability of infiltration." *Water Resour. Res.*, 15(2), 419–429.

Terstriep, M. L., Voorhees, M. L., and Bender, G. M. (1976). "Conventional urbanization and its effect on storm runoff." *Rep. CR-177, Illinois State Water Survey*, Champaign, IL.

Woolhiser, D. A., Smith, R. E., and Giraldez, J. V. (1996). "Effects of spatial variability of saturated hydraulic conductivity on Hortonian overland flow." *Water Resour. Res.*, 32(3), 671–678.

Zheng, F., Huang, C., and Norton, L. D. (2000). "Vertical hydraulic gradient and run-on water and sediment effects on erosion processes and sediment regimes." *Soil Sci. Soc. Am. J.*, 64, 4–11.